A&A 668, A141 (2022)
https://doi.org/10.1051/0004-6361/202243968

Astronomy & Astrophysics

An astrometric mass estimate for asteroid (223) Rosa

M. Kretlow

Instituto de Astrofísica de Andalucía, IAA-CSIC, Glorieta de la Astronomía s/n, 18008 Granada, Spain
e-mail: kretlow@iaa.es

Received 6 May 2022 / Accepted 5 October 2022

ABSTRACT

Context. Outer main belt asteroid (223) Rosa is a possible flyby target of opportunity for the European Space Agency (ESA) JUpiter ICy moons Explorer (JUICE) mission when it passes the asteroid belt on the way to Jupiter. The very low albedo and the featureless red spectra indicate a P-type asteroid in the Tholen taxonomy, though the yet known bulk density does not appear to match this classification.
Aims. The aim of this work is to derive new estimates for the mass and bulk density of (223) Rosa.
Methods. We derived the mass of Rosa by analyzing the gravitational deflection of small "test" asteroids that had a close encounter with Rosa in the past. To find such events suitable for the mass determination, we performed an encounter search with about 900 000 asteroids over the time span 1980–2030.
Results. Three encounters were identified from which two independent mass estimates for Rosa were derived: $M = (5.32 \pm 2.17) \times 10^{17}$ kg and $M = (3.15 \pm 1.14) \times 10^{17}$ kg, respectively. The weighted mean is $M = (3.62 \pm 1.25) \times 10^{17}$ kg. This yields to a bulk density of $\rho = 1.2 \pm 0.5$ g cm^{-3}, when adopting an effective diameter of $D = 83 \pm 8$ km. This bulk density estimate is consistent with typical densities for Tholen taxonomy P-type asteroids.

Key words. minor planets, asteroids: individual: (223) Rosa – astrometry – celestial mechanics – methods: numerical

1. Introduction

Asteroid (223) Rosa (hereafter also Rosa) was recently proposed as a potential ESA JUpiter ICy moons Explorer (JUICE) mission[1] flyby target of opportunity on its way to Jupiter (Avdellidou et al. 2021; Agostini et al. 2022). Rosa is a very dark ($p_V < 0.05$) outer main belt asteroid (proper semi-major axis $a_p = 3.09011$ au)[2], with an effective diameter D of about 83 km (see Sect. 2), of which the composition (e.g., the taxonomic class) and evolution (e.g., the dynamical and collisional history) are still not fully understood.

Important physical parameters characterizing an asteroid are its size and mass, and therefore its bulk density. While diameter estimates do usually exist for an asteroid, provided by at least one of various well-known methods such as radiometry, stellar occultations, and (occultation-)scaled light-curve inversion (3D models), mass estimates are much harder to derive and are known for only a small number (some 10^2) of the known asteroids. Compilations of asteroid masses are available in the literature (e.g., Hilton 2002; Carry 2012, and references therein), and are now also provided by web-based data archives (e.g., Kretlow 2020a).

One of the commonly applied methods in this domain (Hilton 2002) consists in gravitational deflection of a significantly smaller object ("test asteroid") by another asteroid ("perturber") in order to derive the mass of the latter during the mutual encounter. In addition to such investigations, which are used to study individual objects, asteroid masses are also derived as model-parameter fit results in major planetary ephemeris construction (simultaneously with other asteroid masses which are included in the dynamical model). Two mass estimates for Rosa were found in the literature, and both were derived in that way: Fienga et al. (2019) obtained a mass of $M = (5.979 \pm 2.971) \times 10^{17}$ kg. Park et al. (2021) provide a value of $M = 9.350 \times 10^{17}$ kg.

As mentioned, diameter estimates are available for the majority of the known numbered asteroids, as they were observed by dedicated space-based infrared surveys such as performed by the Infrared Astronomical Satellite (IRAS), the Wide-Field Infrared Survey Explorer (WISE), and the Akari satellite, and/or were obtained using other methods, and therefore in many cases more than one size estimate is found in the literature. Using an uncertainty weighted average of $D = 82.7 \pm 8.4$ km for the mean diameter and a mass of $M = (5.979 \pm 2.971) \times 10^{17}$ kg from Fienga et al. (2019), Avdellidou et al. (2021) computed a bulk density of $\rho = 1.79$ g cm^{-3} with a relative uncertainty of about 50%[3].

Section 2 gives an overview of the available size measurements and we aim to provide a (current) best value. In Sect. 3, this work provides a new mass estimate derived from mutual encounters with other small asteroids. Section 4 summarizes the proposed best values for the size and mass of (223) Rosa, provides the resulting bulk density, and discusses these values with respect to the taxonomic class of the asteroid.

2. Diameter estimates

The value (and uncertainty) of the diameter D is crucial for the resulting bulk density due to $\rho \propto D^{-3}$. As mentioned in the introduction, mostly thermal diameters have been published so far.

[1] Currently planned for launch in April 2023.
[2] Proper elements taken from AstDyS, https://newton.spacedys.com/astdys/.
[3] We point out that we derive $\rho = 2.0 \pm 1.2$ g cm^{-3} for these values for D and M.

Table 1. Compilation of literature values for the effective diameter reproduced from Avdellidou et al. (2021) and completed with recent publications.

#	Diameter D (km)	Albedo p_V	Method	Ref.
1	72.33 ± 20.18	0.040 ± 0.050	NEATM	a
2	76.46 ± 29.36	0.035 ± 0.023	NEATM	b
3	79.68 ± 33.85	0.036 ± 0.037	NEATM	c
4	79.81 ± 0.31	0.040 ± 0.010	NEATM	d
5	80.93 ± 1.46	0.037 ± 0.002	NEATM	e
6	83.39 ± 2.97	0.034 ± 0.005	NEATM	f
7	86.05 ± 26.43	0.033 ± 0.046	NEATM	c
8	87.61 ± 4.40	0.031 ± 0.003	STM	g
9	88.50 ± 3.79	0.031 ± 0.003	NEATM	h
10	89.37 ± 3.53	0.030 ± 0.002	STM	h
11	90.43 ± 20.33	0.030 ± 0.020	NEATM	a
12	109.16 ± 0.95	0.020 ± 0.003	NEATM	i
13	72.8 ± 6.3	0.034 ± 0.005	CITPM	j
14	72.5 ± 4.2	0.035 ± 0.005	CITPM	j
15	82.6 ± 8.2	0.032 ± 0.002	c.w. mean	–
16	83.3 ± 8.1	0.033 ± 0.006	evm mean	–

Notes. Two different averages are also provided, the classical weighted (c.w.) mean and the EVM value. Entries with asymmetric uncertainties (entries #13 and #14, reference (j)) are therefore symmetrized (Audi et al. 2017, Appendix A, method 2). Methods: STM (standard thermal model), NEATM (near-Earth asteroid thermal model), CITPM (convex inversion thermophysical model).

References. (a) Nugent et al. (2016), (b) Masiero et al. (2017), (c) Masiero et al. (2020), (d) Masiero et al. (2014), (e) Usui et al. (2011), (f) Masiero et al. (2011), (g) Tedesco et al. (2002), (h) Ryan & Woodward (2010), (i) Masiero et al. (2012), (j) Marciniak et al. (2021).

Table 1 presents the values published up to now. It is out of the scope and beyond the capability of this study to discuss and to evaluate every diameter estimate given in Table 1 in order to identify and argue in favor of a best value. The effective diameter used in this work for Rosa is therefore derived by averaging all these literature values. Because in weighted arithmetic means the error σ is used as weight $w = 1/\sigma^2$, outliers with small formal uncertainties will bias the result. An alternative form of averaging is the expected value method (EVM; Birch & Singh 2014), which is more robust against outliers. Table 1 provides both the traditional weighted average ($D = 82.6 \pm 8.2$ km) and the EVM average ($D = 83.3 \pm 8.1$ km) for the published diameter estimates.

As shown in Fig. 1, Rosa was observed photometrically in different viewing aspects, with Phase Angle Bisector (PAB) longitudes of between 75° and 352°, phase angles α of between 0.9° and 17.1° and aspect angles θ of between 37.6° and 153.8° for pol solution 1 (respectively between 29.3° and 140.5° for pol solution 2) derived by Marciniak et al. (2021). The highest lightcurve amplitude in the set of light curves (Fig. 2) archived at the Centre de Données Stellaires (CDS[4]) is Amax = 0.16 mag for a nearly equatorial view, which corresponds to an axis ratio $a/c = 1.16$ for an aspect angle $\theta = 90°$. The Asteroid Lightcurve Database (LCDB[5]) provides values Amin = 0.06 mag and Amax = 0.13 mag. Putting this together we can expect that Rosa is neither very elongated nor irregular and the assumption of a spherical body made in simple thermal models such as the standard thermal model (STM) or near-Earth asteroid thermal model (NEATM) is appropriate for this asteroid. Averaging all available size estimates derived from STM, NEATM, and also the thermophysical model (TPM) as described above seems reasonable in order to derive a reliable value for the effective diameter.

The observation of stellar occultations by asteroids provides the shape and size of the apparent profile on the sky plane with accuracy to the nearest kilometer. Up to now, three stellar occultations by (223) Rosa were successful observed (Herald et al. 2019): 2004 Sep. 29 (single visual observation with two subsequent occultation events and corresponding chord lengths of 34 km and 78 km, but inconsistent with adjacent negative observations), 2008 May 27 (two chords), and 2014 Apr. 13 (one chord: length = 46.4 km). The 2008 May 27 stellar occultation was recorded by three stations operated by the same observer (i.e., two unattended stations), yielding two positive detections (chord lengths of 54.5 km and 66.7 km) and one negative observation (no occultation detected).

The observation of further stellar (multi-chord) occultations by Rosa will help to refine its volume, especially in combination with light-curve data. Therefore, stellar occultation predictions were performed until the year 2025, considering *Gaia* EDR3 (Early Data Release 3, Brown et al. 2021) stars down to $G = 16$ mag. These predictions will be available on the website[6] of the author. Two upcoming events crossing over Europe (2022 Oct. 7) and the USA (2023 Feb. 24), regions potentially well covered by occultation observers, are presented in Fig. 3.

3. Mass estimates

There are only two mass estimates published in the literature from the construction of planetary ephemerides; just one of these includes error bars (see Sect. 1). The aim of this work is to derive a new estimate for the mass of Rosa by means of a gravitational deflection analysis.

In a first step, a search for suitable test asteroids was performed essentially by integrating (223) Rosa and about 900 000 known asteroids[7] backwards until the year 1980 (and also into the future until the year 2030 in order to identify upcoming events). If the euclidean distance between Rosa and another (test) asteroid became smaller than 0.05 au during this ephemeris interval, the mutual encounter was stored together with additional information such as the time span of available observations of the test asteroid, the relative encounter velocity, and the parameter $P = D_1^3/(r\,v)$; with D_1 the diameter of the perturber (set to $D_1 = 83 \pm 8$ km; see Sect. 2), r the encounter distance between both objects in km, and v their relative encounter velocity in km s^{-1}. P is a proxy for the change in the mean motion Δn of the perturbed body (Galád 2001). This resulting list of encounters was finally used to select candidates for the asteroid mass determination. For (223) Rosa, three close encounters were identified to be potentially suitable for the mass determination (Table 2).

The mass M of the perturbing body (Rosa) was determined by means of a least-squares fit of the solve-for parameters to the astrometric observations[8] of the test asteroid by solving the

[4] http://cdsarc.u-strasbg.fr/viz-bin/cat/J/A+A/654/A87

[5] https://www.minorplanet.info/PHP/lcdb.php

[6] https://astro.kretlow.de/cora/occultations

[7] Orbital elements taken from MPC's MPCORB.DAT (https://www.minorplanetcenter.net/iau/MPCORB.html).

[8] Provided by the Minor Planet Center (MPC, https://www.minorplanetcenter.net/).

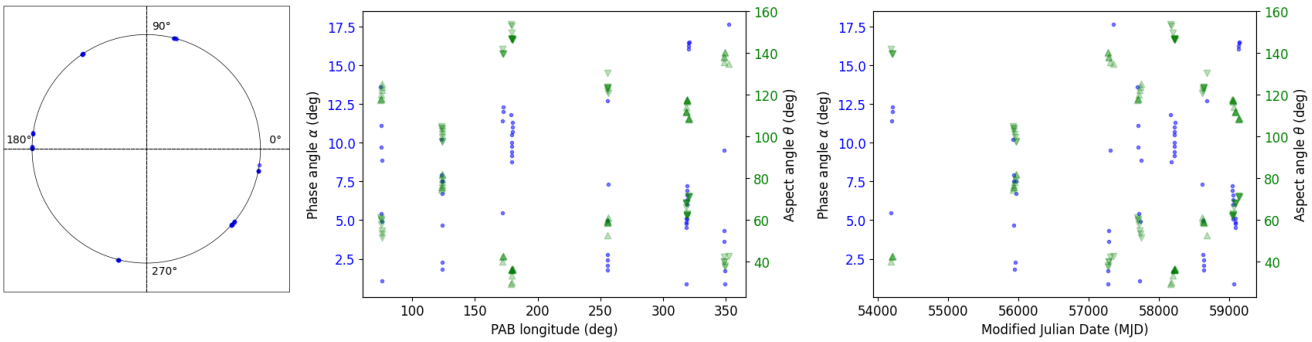

Fig. 1. Aspect data for the light curves given in Fig. 2. The *left panel* shows the PAB longitude distribution. In the *middle* and *right panel* the phase and aspect angle α, θ are given as a function of PAB longitude (*middle*) and MJD (*right*). The phase angle α is marked with dots. The aspect angle θ is computed for both solutions derived by Marciniak et al. (2021). Solution $\lambda_p, \beta_p = (22°, 18°)$ is marked by triangles (▲), the mirror solution $\lambda_p, \beta_p = (203°, 26°)$ by upside-down triangles (▼).

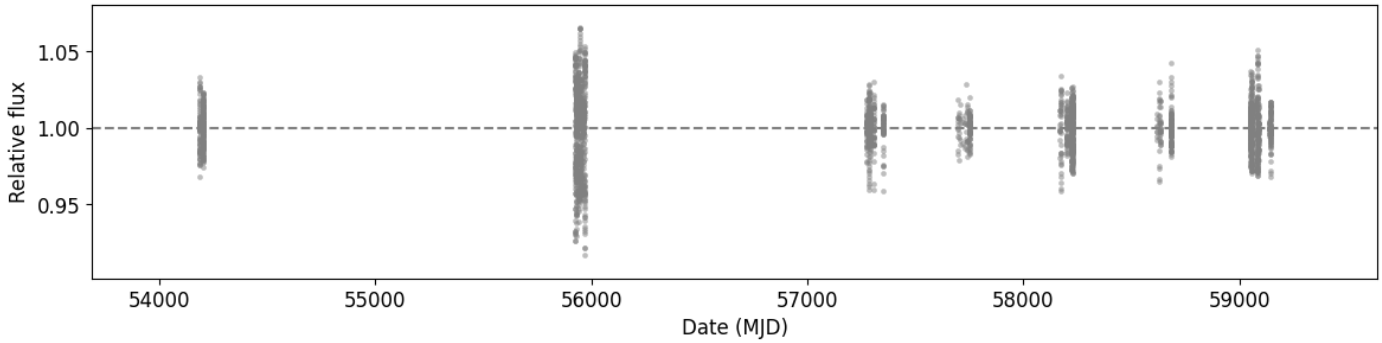

Fig. 2. Overview of all 58 currently available optical light curves archived at the CDS (http://cdsarc.u-strasbg.fr/viz-bin/cat/J/A+A/654/A87, Marciniak et al. 2021). Given is the relative brightness (in intensity units) normalized to the mean brightness vs time (MJD) for the time span 2007–2020. The maximum amplitude Amax for the epoch around MJD 55950 is 0.16 mag and corresponds to a nearly equatorial view; see Fig. 1 (*right panel*). The LCDB (https://www.minorplanet.info/PHP/lcdb.php) provides the values Amin = 0.06 mag and Amax = 0.13 mag.

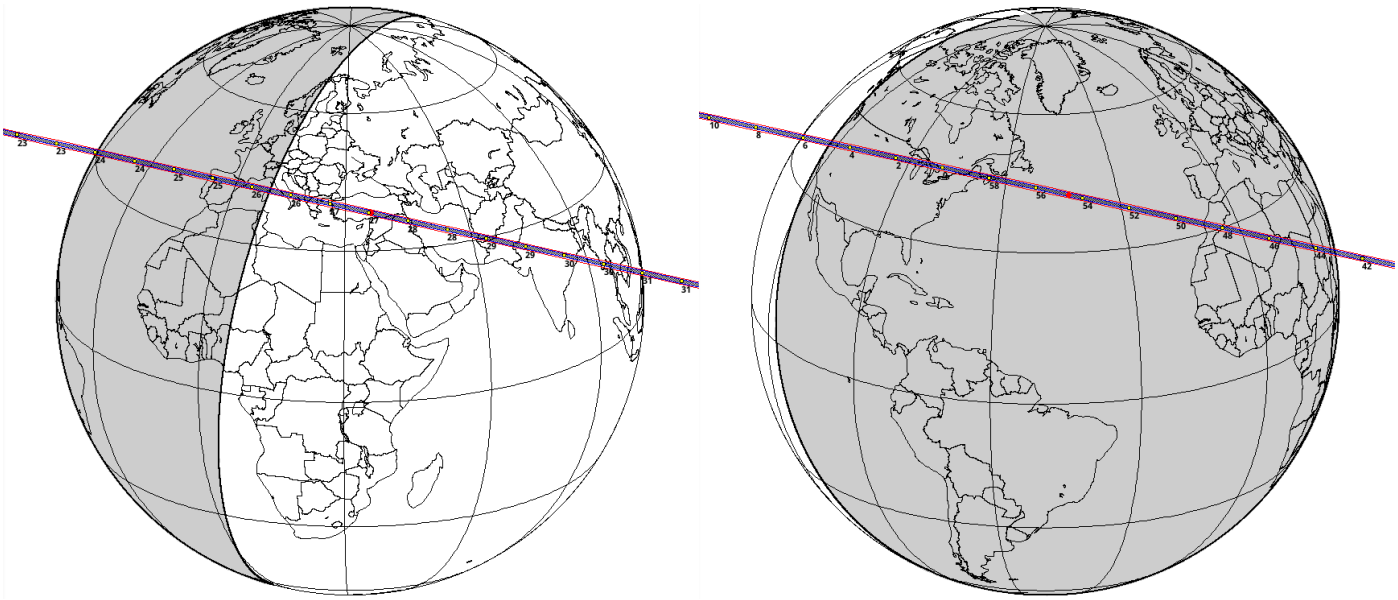

Fig. 3. Two stellar occultation predictions for (223) Rosa. The red line marks the $1-\sigma$ cross-track uncertainty (about 24 km for both events). Minute time ticks are marked with yellow dots. The time of geocentric closest approach (c.a.) is marked by the red dot. *Left-hand side*: occultation of the star *Gaia* EDR3 0664382207483343488 on 2022 Oct. 7 at 05:27:31 UT (c.a.), visible in Portugal and Spain (though twilight will interfere in the eastern part of Spain). The star has $G = 13.5$ mag, the expected magnitude drop will be 2.0 mag, the maximum duration about 2.9 s. *Right-hand side*: occultation of the star *Gaia* EDR3 0661647103588763776 on 2023 Feb. 24 at 01:54:39 UT (c.a.), visible in the U.S. and northern Africa (Morocco, Algeria, etc.) The star has $G = 13.9$ mag, the expected magnitude drop will be 0.8 mag, and the maximum duration about 9.6 s.

Table 2. Test asteroids and their mutual encounter events used for the mass determination of (223) Rosa, ordered by encounter date.

Test asteroid	Encounter date	r au	v km s^{-1}	D_2 km	P km s	Obs. arc yyyy.mm	M_{223} 10^{17} kg
(78824) 2003 QS13	2001-06-26.93	0.0002	2.837	1.8	8.1 ± 2.3	1960.09 – 2021.12	–
(35525) 1998 FV64	2010-12-31.87	0.0004	2.043	3.9	5.3 ± 1.5	1990.09 – 2021.11	5.32 ± 2.17
(315162) 2007 FL24	2016-07-04.05	0.0027	0.131	1.8	12.3 ± 3.5	1999.11 – 2021.11	3.15 ± 1.14

Notes. Given are the designation of the test asteroid, the date of the encounter, the minimum Euclidean distance r between Rosa and the test asteroid, the relative encounter velocity v, the diameter D_2 of the test asteroid (either taken from the orbital elements file astorb.dat (https://asteroid.lowell.edu/main/astorb/) or calculated from the absolute magnitude H), the perturbation parameter P, the time span covered by the astrometric observations filed at the MPC (https://www.minorplanetcenter.net/, at date 2021 Dec. 10), and the derived mass value M_{223} for Rosa.

Table 3. List of perturbing asteroids included in the dynamical model.

Asteroid	Mass (kg)	Asteroid	Mass (kg)
(1) Ceres	9.38×10^{20}	(16) Psyche	2.29×10^{19}
(2) Pallas	2.05×10^{20}	(29) Amphitrite	1.33×10^{19}
(3) Juno	2.63×10^{19}	(52) Europa	2.34×10^{19}
(4) Vesta	2.59×10^{20}	(65) Cybele	1.63×10^{19}
(6) Hebe	1.28×10^{19}	(87) Sylvia	1.51×10^{19}
(7) Iris	1.41×10^{19}	(88) Thisbe	1.03×10^{19}
(10) Hygiea	8.42×10^{19}	(511) Davida	3.08×10^{19}
(15) Eunomia	3.16×10^{19}	(704) Interamnia	3.54×10^{19}

Notes. The masses of the asteroids are taken from (Kretlow 2020a,b).

system of linear equations:

$$P\Delta E + Q\Delta M = R, \tag{1}$$

where $P = \partial(\alpha, \delta)/\partial E$ is the matrix of partial derivatives of the observed coordinates (α, δ) with respect to the six initial values $E_1, \ldots, E_6$ (position and velocity) of the test asteroid. $Q = \partial(\alpha, \delta)/\partial M$ is the matrix of partial derivatives of the observed coordinates of the test asteroid with respect to the perturbing mass M, and R is the matrix depending on the (O–C) residuals in coordinates of the test asteroid. $\Delta E = (\Delta E_1, \ldots, \Delta E_6)$ are the corrections to the six initial values of the test asteroid and ΔM is the correction to the mass of the perturbing body. The partial derivatives P, Q were not computed by numerical variation, but rather by integrating a set of seven differential equations together with the equations of motion of the test asteroid (Sitarski 1971).

The numerical integration was carried out using a multistep, variable-order, predictor–corrector (PECE) method with self-adjusting step size (Shampine & Gordon 1975). The masses of the planets and their state vector during the integration were read from an external file (JPL DE440). The perturbing asteroids of the dynamical model were handled in a similar way, as was the perturber Rosa. The ephemerides of all of these objects are precomputed and stored as Chebyshev polynomials in external files, to be used in the program on demand. The perturbing asteroids are summarized in Table 3. If applicable, those astrometric observations of the test asteroid which were reduced with non-Gaia star catalogs, were de-biased (Eggl et al. 2020). For the weights of the observations during the differential orbit correction of the test asteroid, the error estimates given by Veres et al. (2017) were used.

(35525) 1998 FV64. This encounter between 1998 FV64 and Rosa at the end of the year 2010 has the smallest perturbation parameter value of all three events presented here. The pre-encounter as well as post-encounter observation coverage is extensive and homogeneous. A mass estimate $M = (5.32 \pm 2.17) \times 10^{17}$ kg was derived for Rosa.

(315162) 2007 FL24. 2007 FL24 had a long and slow encounter with Rosa in 2016 (showing the largest perturbation parameter P of all three cases), and also good astrometric coverage both pre-encounter and post-encounter. The orbit solution for this encounter yields a mass estimate $M = (3.15 \pm 1.14) \times 10^{17}$ kg.

Because the osculating orbital elements of Rosa and 2007 FL24 appear very similar, the possibility of being an asteroid pair was investigated. First, the distance between them in the three-parameter space was calculated using their proper elements[9] and the formula (Zappala et al. 1990):

$$d = na\sqrt{k_a(\Delta a/a)^2 + k_e(\Delta e)^2 + k_i(\Delta \sin i)^2}, \tag{2}$$

with a the mean of both semi-major axes, n the corresponding mean motion, and the standard metric weighting factors $k_a = 5/4, k_e = k_i = 2$. Though the high value of $d = 51\,\mathrm{m\,s^{-1}}$ made it unlikely that these two bodies are an asteroid pair, a 500 kyr backward integration was made using the mercury6 software (Chambers 2012) regarding all major planets (M-N) plus the dwarf planet or asteroids Ceres, Pallas, and Vesta, but without applying any non-gravitational forces. No close encounter or coincidence point was found in this time span, and therefore the orbital similarity seems to be a random coincidence.

(78824) 2003 QS13. Though this encounter in 2001 has a perturbation parameter $P = 8.1 \pm 2.3$ km s, which is even larger than that of the interaction with 1998 FV64, the orbit solution did not yield a physically reasonable mass solution for Rosa. A likely explanation is that only four pre-encounter nights of observation are available, one night in September 1960 (Palomar Mountain, 675), one single observation in 1994 (Tautenburg, 033), and two sequential nights in December 1996 (Prescott, 684). A re-reduction of these pre-encounter observations (if available) using the Gaia star catalog could be helpful. A search in image archives[10] to retrieve additional and precise positions was not successful, because the object was usually too faint to be detected on older survey images such as NEAT (Near-Earth Asteroid Tracking) GEODSS/Maui. Table 4 lists the images that

[9] Provided by AstDyS (https://newton.spacedys.com/astdys/).

[10] Using the CADC Solar System Object Image Search (SSOIS, https://www.cadc-ccda.hia-iha.nrc-cnrc.gc.ca/en/ssois/index.html).

Table 4. Archived survey images on which the asteroid (78824) 2003 QS13 would have potentially been observed.

Image	MJD	Exp.(s)	Telescope/instrument	Datalink
961217104449a	50434.4477893518	40	NEAT-GEODSS-Maui	<url-prefix>/g19961217/obsdata/961217104449a.fit.fz
961217105739a	50434.4567013889	40	NEAT-GEODSS-Maui	<url-prefix>/g19961217/obsdata/961217105739a.fit.fz
961217110944a	50434.4650925926	40	NEAT-GEODSS-Maui	<url-prefix>/g19961217/obsdata/961217110944a.fit.fz
970111053115a	50459.2300347222	40	NEAT-GEODSS-Maui	<url-prefix>/g19970111/obsdata/970111053115a.fit.fz
970111054321a	50459.2384375000	40	NEAT-GEODSS-Maui	<url-prefix>/g19970111/obsdata/970111054321a.fit.fz
970111055852a	50459.2492129630	40	NEAT-GEODSS-Maui	<url-prefix>/g19970111/obsdata/970111055852a.fit.fz
980326100223a	50898.4183217593	20	NEAT-GEODSS-Maui	<url-prefix>/g19980326/obsdata/980326100223a.fit.fz
980326101659a	50898.4284606481	20	NEAT-GEODSS-Maui	<url-prefix>/g19980326/obsdata/980326101659a.fit.fz
980326101920a	50898.4300925926	20	NEAT-GEODSS-Maui	<url-prefix>/g19980326/obsdata/980326101920a.fit.fz
980326103127a	50898.4385069444	20	NEAT-GEODSS-Maui	<url-prefix>/g19980326/obsdata/980326103127a.fit.fz
980326103353a	50898.4401967593	20	NEAT-GEODSS-Maui	<url-prefix>/g19980326/obsdata/980326103353a.fit.fz
980326104827a	50898.4503125000	20	NEAT-GEODSS-Maui	<url-prefix>/g19980326/obsdata/980326104827a.fit.fz
980327100349a	50899.4193171296	20	NEAT-GEODSS-Maui	<url-prefix>/g19980327/obsdata/980327100349a.fit.fz
980428081456a	50931.3437037037	20	NEAT-GEODSS-Maui	<url-prefix>/g19980428/obsdata/980428081456a.fit.fz
980428084448a	50931.3644444444	20	NEAT-GEODSS-Maui	<url-prefix>/g19980428/obsdata/980428084448a.fit.fz
980428091458a	50931.3853935185	20	NEAT-GEODSS-Maui	<url-prefix>/g19980428/obsdata/980428091458a.fit.fz
980525060228a	50958.2517129630	20	NEAT-GEODSS-Maui	<url-prefix>/g19980525/obsdata/980525060228a.fit.fz
980525063130a	50958.2718750000	20	NEAT-GEODSS-Maui	<url-prefix>/g19980525/obsdata/980525063130a.fit.fz
980525070207a	50958.2931365741	20	NEAT-GEODSS-Maui	<url-prefix>/g19980525/obsdata/980525070207a.fit.fz

Notes. The limiting magnitude on these images is typically around 18 mag for 20 s and 19 mag for 30 s exposure times (Exp.) respectively, depending on sky conditions etc. The asteroid could not be detected on any of these images as the object was usually too faint (between 20 V-mag and 22 V-mag), with the exception of the date 1996 Dec 17, where the asteroid was at a predicted 19.3 V-mag. However, the asteroid was not found on those images either. MJD = JD–2400000.5 is the Modified Julia Date of the start of the exposure. The <url-prefix> is https://sbnarchive.psi.edu/pds3/neat/geodss

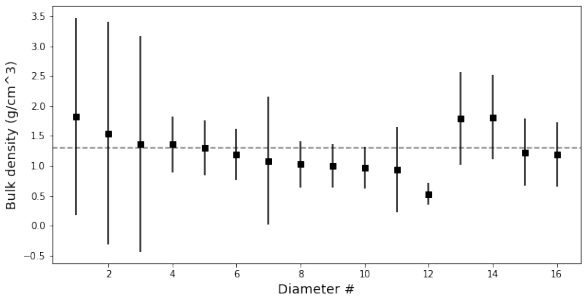

Fig. 4. Bulk density as a function of the diameters given in Table 1 for the final mass estimate $M = (3.62 \pm 1.25) \times 10^{17}$ kg. The horizontal dashed line marks the typical density $\rho \approx 1.3\,\mathrm{g\,cm^{-3}}$ for Tholen taxonomy P-type asteroids.

were examined for this asteroid. It is also conceivable that a different numerical approach, such as a Monte Carlo parameter estimation (Siltala & Granvik 2020), might be able to use this encounter for a mass determination with the existing astrometry. A summary of all three encounter circumstances and the derived mass results is given in Table 2.

4. Results and discussion

From two individual close encounters with small asteroids, we estimated the mass of Rosa to be $M = (5.32 \pm 2.17) \times 10^{17}$ kg and $M = (3.15 \pm 1.14) \times 10^{17}$ kg, respectively. The weighted mean value is $M = (3.62 \pm 1.25) \times 10^{17}$ kg. Figure 4 shows the bulk density as a function of the diameters given in Table 1. By adopting $D = 83.3 \pm 8.1$ km as the (currently) best value for the diameter, the corresponding bulk densities are $\rho = 1.8 \pm 0.9\,\mathrm{g\,cm^{-3}}$ and $\rho = 1.0 \pm 0.5\,\mathrm{g\,cm^{-3}}$. The weighted mean is $\rho = 1.2 \pm 0.5\,\mathrm{g\,cm^{-3}}$. The EVM mean of the visual albedo is $p_V = 0.033 \pm 0.006$.

The mass values derived in this work are smaller than the values $M = (5.979 \pm 2.971) \times 10^{17}$ kg and $M = 9.350 \times 10^{17}$ kg (Fienga et al. 2019; Park et al. 2021), which yield bulk densities of $\rho = 2.0 \pm 1.1\,\mathrm{g\,cm^{-3}}$ and $\rho = 3.1\,\mathrm{g\,cm^{-3}}$, respectively.

From the reassessment of the existing spectra and spectrophotometric data, supplemented with their own near-infrared and visible spectra taken in 2021 and the very low albedo, Avdellidou et al. (2021) concluded that Rosa is probably a Tholen taxonomy P-type asteroid, though the previously mentioned densities of $2.0 \pm 1.1\,\mathrm{g\,cm^{-3}}$ and $3.1\,\mathrm{g\,cm^{-3}}$ would be somewhat too large for this taxonomic class.

However, the bulk density $\rho = 1.2 \pm 0.5\,\mathrm{g\,cm^{-3}}$ that we obtain for Rosa agrees well with typical densities of P-type asteroids, such as (87) Sylvia and (107) Camilla ($\rho \approx 1.3\,\mathrm{g\,cm^{-3}}$; see e.g., Carry et al. 2021; Vernazza et al. 2021).

Acknowledgements. The occultation observations made by Roger Venable (USA), provided by the International Occultation Timing Association (IOTA) and by Herald et al. (2019) are acknowledged. Also appreciated are the services and data provided by the Asteroids Dynamic Site (AstDys), JPL Horizon and the Minor Planet Center (MPC). This work has made use of data from the European Space Agency (ESA) mission *Gaia* (https://www.cosmos.esa.int/gaia), processed by the Gaia Data Processing and Analysis Consortium (DPAC, https://www.cosmos.esa.int/web/gaia/dpac/consortium). The author thanks the referee for the helpful comments and constructive review of the paper. I also like to thank Anna Marciniak (A. Mickiewicz University, Poznan, Poland) for her comments on their work and results on (223) Rosa and José Luis Ortiz (IAA, Granada, Spain) for reading and commenting the original manuscript. Finally I like to acknowledge open-source software and tools, like Linux, Julia + Packages, Jupyter, Python + Packages, Gnuplot, GNU Fortran, SQLite, GSHHG (shorelines DB), etc.

References

Agostini, L., Lucchetti, A., Pajola, M., et al. 2022, Planet. Space Sci., 216, 105476

Audi, G., Kondev, F. G., Wang, M., Huang, W., & Naimi, S. 2017, Chinese Phys. C, 41, 030001
Avdellidou, C., Pajola, M., Lucchetti, A., et al. 2021, A&A, 656, A18
Birch, M., & Singh, B. 2014, Nuclear Data Sheets, 120, 106
Brown, A. G. A., Vallenari, A., Prusti, T., et al. 2021, A&A, 649, A1
Carry, B. 2012, Planet. Space Science, 73, 98
Carry, B., Vernazza, P., Vachier, F., et al. 2021, A&A, 650, A129
Chambers, J. E. 2012, Astrophysics Source Code Library, [record ascl:1201.008]
Eggl, S., Farnocchia, D., Chamberlin, A. B., & Chesley, S. R. 2020, Icarus, 339, 113596
Fienga, A., Deram, P., Viswanathan, V., et al. 2019, Notes Scientifiques et Techniques de l'Institut de Mecanique Celeste, 109
Galád, A. 2001, A&A, 370, 311
Herald, D., Frappa, E., Gault, D., et al. 2019, Asteroid Occultations V3.0, Tech. rep., NASA Planetary Data System
Hilton, J. L. 2002, Asteroid Masses and Densities, Asteroids III ADS, 103
Kretlow, M. 2020a, Size, Mass and Density of Asteroids (SiMDA) - A Web Based Archive and Data Service, Tech. Rep., EPSC2020-690, Copernicus Meetings
Kretlow, M. 2020b, https://doi.org/10.5281/zenodo.4039774
Marciniak, A., Durech, J., Ali-Lagoa, V., et al. 2021, A&A, 654, A87
Masiero, J. R., Mainzer, A. K., Grav, T., et al. 2011, ApJ, 741, 68
Masiero, J. R., Mainzer, A. K., Grav, T., et al. 2012, ApJ, 759, L8
Masiero, J. R., Grav, T., Mainzer, A. K., et al. 2014, ApJ, 791, 121
Masiero, J. R., Nugent, C., Mainzer, A. K., et al. 2017, AJ, 154, 168
Masiero, J. R., Mainzer, A. K., Bauer, J. M., et al. 2020, Planet. Sci. J., 1, 5
Nugent, C. R., Mainzer, A., Bauer, J., et al. 2016, AJ, 152, 63
Park, R. S., Folkner, W. M., Williams, J. G., & Boggs, D. H. 2021, AJ, 161, 105
Ryan, E. L., & Woodward, C. E. 2010, AJ, 140, 933
Shampine, L., & Gordon, M. 1975, Computer Solution of Ordinary Differential Equations: The Initial Value Problem (San Francisco: W. H. Freeman and Co.)
Siltala, L., & Granvik, M. 2020, A&A, 633, A46
Sitarski, G. 1971, Acta Astron., 21, 87
Tedesco, E. F., Noah, P. V., Noah, M., & Price, S. D. 2002, AJ, 123, 1056
Usui, F., Kuroda, D., Müller, T. G., et al. 2011, PASJ, 63, 1117
Veres, P., Farnocchia, D., Chesley, S. R., & Chamberlin, A. B. 2017, Icarus, 296, 139
Vernazza, P., Ferrais, M., Jorda, L., et al. 2021, A&A, 654, A56
Zappala, V., Cellino, A., Farinella, P., & Knezevic, Z. 1990, AJ, 100, 2030